



EXPLORING FeMnVAI HEUSLER ALLOY: PHYSICAL, MECHANICAL, AND MAGNETIC PROPERTIES

R. B. Ray^{1,2}, R. K. Rai¹, D. K. Yadav³, G. C. Kaphle^{1,*}

¹Central Department of Physics, Tribhuvan University, Kirtipur, Kathmandu, Nepal

²Amrit Campus, Tribhuvan University, Thamel, Kathmandu, Nepal

³Department of Physics and Astronomy, University of Utah, SLC, Utah, 84102, USA

*Corresponding Email: gopi.kaphle@cdp.tu.edu.np; gck223@gmail.com

Received: 2nd Oct., 2023

Revised: 14th Jan., 2024

Accepted: 22nd Jan, 2024

Abstract

The structural, mechanical, electronic, and magnetic properties of equiatomic quaternary Heusler alloy FeMnVAI have been investigated using first-principles approach. This alloy shows ferromagnetic ground state structure with chemical stability indicating compound fulfills the criteria for synthesizing experimentally. The calculated values of Pugh's index and Poisson's ratio confirmed ductile nature of FeMnVAI. The investigation of band structure and density of states validates the behaviour of half-metallic ferromagnets (HMFs), which follow the Slater-Pauling rule $M_t = Z_t - 24$ and have a magnetic moment value of around $1 \mu_B/\text{f.u.}$ Its features also allow for potential applications in the realm of spintronics devices and optoelectronics.

Keywords: DFT, Quaternary Heusler alloy, HMFs, Slater-Pauling rule, Spintronics

I. INTRODUCTION

R. A. de Groot et al. reported half-metallic ferromagnet (HMF) in half-Heusler alloy NiMnSb for the first time in 1983 [1]. Subsequently, half-metallic ferromagnets (HMFs) have drawn increasing attention as promising materials for electronic devices, such as tunnel junctions and spin valves [2–6]. Numerous theoretical efforts have been made to use first principles calculations to anticipate novel HMFs in Heusler alloys and other material systems [7, 8]. One spin channel in the electronic structure of HM alloy exhibits metallic behaviour, while the second spin

channel, which has a band gap at the Fermi level (E_F), exhibits semiconducting features. These substances possess conduction electrons with 100% spin polarisation, resulting in an integer spin magnetic moment per formula unit.

The Heusler alloy is an excellent material system with several useful features, including phase change, superconducting, thermoelectric, topological, HM, and spin gapless properties. It has been discovered through theoretical and experimental research that Heusler alloys containing 3d transition elements—such as those based on Mn, Fe, Co, Cr, Ni, V, and Ru—have been successfully synthesised on a large scale

[9–11]. The full Heusler alloys Mn_2CoZ ($Z = Al, Ga, Si, Sb$), Co_2CrGa , Fe_2CoSi , $Co_2Mn_{1-x}Fe_x$ and quaternary Heusler alloys $FeCoCrSi$, $CoFeMnSi$, have been explored to contain HM character by both practical and theoretical research [12-14]. Strain, tension, flaws, and temperature can readily destroy a small HM band gap in the HM materials. Therefore, it is crucial to look for novel materials with a wide HM band gap for use in spintronic device applications. Heusler alloys generally fall into one of three categories: (i) Half-Heusler alloy with structure XYZ that crystallises in space group F-43m in C1b configuration [15–18]. (ii) Full-Heusler alloy, crystallising in the $L2_1$ structure with space group $Fm\bar{3}m$ and chemical formula X_2YZ [19–22]. and (iii) the quaternary Heusler alloy, which crystallises in a Y-type structure with space group F-43m, and has the formula $XX'YZ$ [23–28], where Z is the main group s and p elements, whereas X, X', and Y are transition metal (TM) elements. We here are investigating the important properties of third group of Heusler systems.

Zhang et al. investigated the half-metallic properties of quaternary Heusler alloys, specifically $NbVMnAl$ and $NbFeCrAl$, using first principles. They found that these alloys exhibit half metallic properties with certain band gaps in opposite spin channels following Slater-Pauling rules $M_t = Z_t - 24$ and $M_t = Z_t - 21$, respectively [29]. Dia et al. conducted theoretical studies on three superstructures of the

quaternary Heusler alloy $CoFeMnSi$. They observed that the first superstructure displays half-metallicity, the second one has a pseudogap at the Fermi level, and the third indicates metallic behavior. However, experimental analysis, including X-ray diffraction (XRD) pattern and magnetization curve measurements, confirmed that $CoFeMnSi$ crystallizes in the first structure exhibiting half-metallicity [30]. Out of the $CoCuMnZ$ ($Z=In, Sn, and Sb$) Quaternary Heusler compounds, $CoCuMnIn$ and $CoCuMnSn$ are observed as metallic whereas $CoCuMnSb$ is a real half-metal with an indirect band gap at one spin channel[31]. Comparably, it was discovered that the compounds $MnCoMoAl$ and $MnTiMoAl$ were ferrimagnetic (FIM) in the ground state, with half-metallic and metallic characteristics respectively. Furthermore, the magnetic moments do not change even when strain is applied between -12% and +12% range [32]. Recent study on Zr-based equiatomic quaternary Heusler alloys $ZrRhTiZ$ ($Z = Al, In$) predicted that the uniform strain on half-metallicity inverts the band gap from one spin state to another spin state [33].

Here, we are investing the mechanical, agnetic, and other related physical properties of the $FeMnVAl$ quaternary Heusler alloy using the GGA, mBJ, and GGA+U techniques. The half-metallic behaviour of the $FeMnVAl$ system is described by all methods. Applying the GGA +U and mBJ methods enhance the small half-metallic gap over GGA. This unique characteristic

distinguishes this study from others.

II. COMPUTATIONAL DETAILS

The electronic structure calculations were conducted using density functional theory (DFT) based first-principle approach implemented in the WIEN2k code [46-48]. To address issues like underestimation of band gaps by generalized gradient approximation (GGA) [34-36]. We employed the modified Becke-Johnson (mBJ) potential [37, 38] along with the GGA+U approach [39, 40]. The mBJ potential provides better treatment of d-electrons, while GGA+U incorporates a Hubbard potential (U) to accurately describe highly correlated systems containing transition metals (Fe, Mn, V). Specifically, U values of 0.89 eV, 0.64 eV, and 0.61 eV were used for Fe, Mn, and V respectively. This combination ensures more precise electronic structure calculations for the materials under study. To ensure accurate convergence, we set a cutoff energy of -6 Ry and a $17 \times 17 \times 17$ mesh (equivalent to 5000 k-points) for SCF calculations. The structural optimization and SCF calculations are achieved until the

energy change per atom is less than 10^{-7} eV and charge convergence is 10^{-4} electrons. Crystal structures were visualized with VESTA, and figures were plotted using Xmgrace. Elastic results were collected using IRelast 14.1 [41].

III. RESULTS AND DISCUSSION

A: Structural, chemical and mechanical stability

The equiatomic quaternary Heusler alloy FeMnVAI crystallizes into a Y-type structure with space group F-43m (space group number 216) [42, 43]. This structure comprises four interpenetrating sublattices distributed across four Wyckoff positions (4a, 4b, 4c, 4d) [44-47]. Three arrangement modes, namely type I, type II, and type III, exist based on the occupation of Fe, V, and Al atoms at specific crystal sites, while Mn occupies another site (Table 1). Our computations involved optimizing these structures in both nonmagnetic (NM) and ferromagnetic (FM) states. The results show that the type I structure in the FM state exhibits the lowest energy, indicating its greater stability compared to other structures in NM states (Fig. 1).

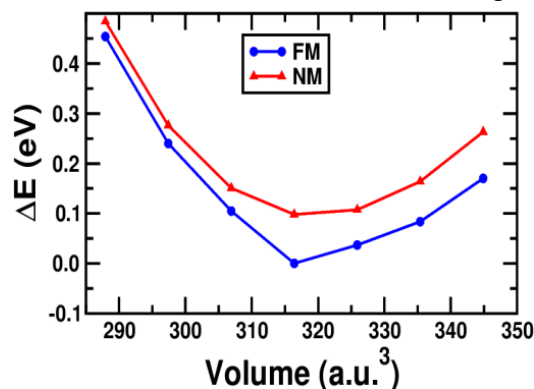


Figure 1. (Color online) The structural volume optimization of quaternary Heusler compound FeMnVAI in non-magnetic and ferromagnetic states.

TABLE I. The atomic sites occupation of FeMnVAI compound in distinct arrangement modes.

Type	4a(0, 0, 0)	4b(0.25, 0.25, 0.25)	4c(0.5, 0.5, 0.5)	4d(0.75, 0.75, 0.75)
Type I	Al	Fe	V	Mn
Type II	Al	V	Fe	Mn
Type III	V	Al	Fe	Mn

The Birch-Murnaghan equation of state (EOS) has yielded the optimised value of the lattice parameter following the completion of all optimisation procedures. The EOS is given as [48],

$$E = E_0(V) + \frac{BV}{B'(B-1)} \left[B \left(1 - \frac{V_0}{V} \right) + \left(\frac{V_0}{V} \right)^B - 1 \right] \quad (1)$$

Where E_0 and V_0 are the minimum equilibrium energy and volume, B is the bulk modulus, B' is the derivative of the bulk modulus. Plot shows that that the optimized lattice parameter of FeMnVAI alloy is 5.757\AA . The optimized schematic structure is shown in Fig. 2.

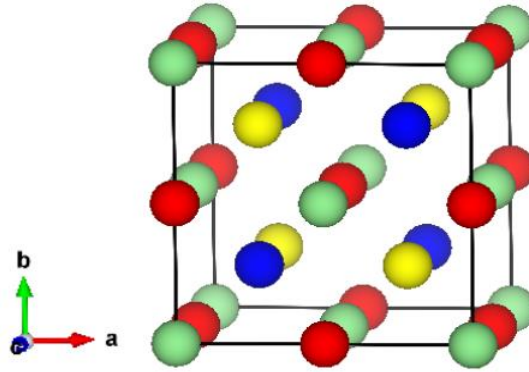


FIG. 2. (Color online) Schematic crystal structure representation of quaternary Heusler compound FeMnVAI (Fe = yellow, Mn = blue, V = red, Al = green)

The cohesive and formation energies are computed to show the chemical stability of the compound. It is possible to express the cohesive and formation energies for the FeMnVAI compound as [49, 50]

$$E_{for} = E_{FeMnVAI}^{total} - (E_{Fe}^{bulk} + E_{Mn}^{bulk} + E_{V}^{bulk} + E_{Al}^{bulk}) \quad (2)$$

$$E_{coh} = E_{FeMnVAI}^{total} - (E_{Fe}^{iso} + E_{Mn}^{iso} + E_{V}^{iso} + E_{Al}^{iso}) \quad (3)$$

Here, E_{for} and E_{coh} represents formation and

cohesive energies of the compound and total energy per formula unit is represented by $E_{FeMnVAI}^{total}$. E_{Fe}^{bulk} , E_{Mn}^{bulk} , E_{V}^{bulk} , E_{Al}^{bulk} denote the total energy per atom for Fe, Mn, V, Al in bulk form whereas, E_{Fe}^{iso} , E_{Mn}^{iso} , E_{V}^{iso} , E_{Al}^{iso} stand the total energy of the corresponding single isolated atom, respectively.

The investigated values of formation and

cohesive energies of FeMnVAI are -0.535 eV/atom and -5.325 eV/atom respectively, indicating that compound shows chemical stability. Both structural and chemical stability ensures that the compound can also be synthesized experimentally.

Similarly, we simply require the three independent elastic constants C_{11} , C_{12} , and C_{44} to determine the mechanical properties of this cubic compound. In order to study these elastic constants without changing the system's overall volume, the strain is used. Born and Huang have articulated [51, 52], the conventional mechanical stability standards for cubic crystal as follows:

$$C_{11} - C_{12} > 0, C_{11} > 0, C_{44} > 0, C_{11} + 2C_{12} > 0, \\ C_{12} < B < C_{11} \quad (4)$$

The considered alloy becomes stable if these

stability conditions are satisfied by elastic constants otherwise the alloy is unstable. The computed values of elastic constants C_{11} , C_{12} and C_{44} are tabulated in table-III. From the table, it is observed that all elastic constants have positive values and meet all the mechanical stability conditions. Hence, the compound (FeMnVAI) is mechanically stable against deformation. The compressibility of materials can be measured by measuring bulk modulus B, which is computed by using the relation,

$$B = \frac{1}{3}(C_{11} + 2C_{12}) \quad (5)$$

The value of bulk modulus obtained from the Birch-Murnaghan equation of state for the compound FeMnVAI is 206.19 GPa which is nearly close to the bulk modulus calculated using the elastic constants (table-II).

TABLE II: The investigated elastic constants C_{11} , C_{12} , C_{44} (GPa) and moduli in GPa for FeMnVAI compound

Alloy	C_{11}	C_{12}	C_{44}	B	G	E	B/G	N
FeMnVAI	420.80	200.10	132.80	273.67	123.32	321.65	2.21	0.30

The stiffness of materials are predicted by measuring its shear modulus G. The average value of G can be obtained by using the Hill approximation as [66],

$$G = \frac{1}{2}(G_R + G_V) \quad (6)$$

Where

$$G_V = \frac{1}{5}(C_{11} - C_{12} + 3C_{44}) \quad (7)$$

$$G_R = \frac{5}{3} \frac{(C_{11} - C_{12})C_{44}}{(C_{11} - C_{12}) + 4C_{44}} \quad (8)$$

Here, subscripts V and R represents Voigt and Reuss bounds in G_V and G_R respectively.

The ratio of linear stress to strain gives the measure of Young's modulus E. The increase in value of E increases the covalent property of the material and therefore, affects the ductility. In terms of bulk modulus B and shear modulus G,

the Young's modulus E can be written as,

$$E = \frac{9BG}{3B+G} \quad (9)$$

The ductility or brittleness of materials can be determined by another parameter called Poisson's ratio ν given by the following equation as

$$\nu = \frac{3B-2G}{2(3B+G)} \quad (10)$$

The material is ductile if its Poisson's value is greater than critical value 0.26, otherwise the material is brittle. The calculated value of ν for the compound is 0.30 showing ductile nature.

Similarly the positive value of Cauchy pressure ($C_P = C_{11} - C_{44}$) and the Pugh's index (B/G) value (2.21 greater than critical value 1.75) confirms the ductile nature of FeMnVAI compound.

B: Electronic properties

Analysis of the density of states (DOS) and electronic band structure is crucial to understand the electronic characteristics. The band structure and DOS plot of FeMnVAI using the GGA method are displayed in Figure 3(a,b).

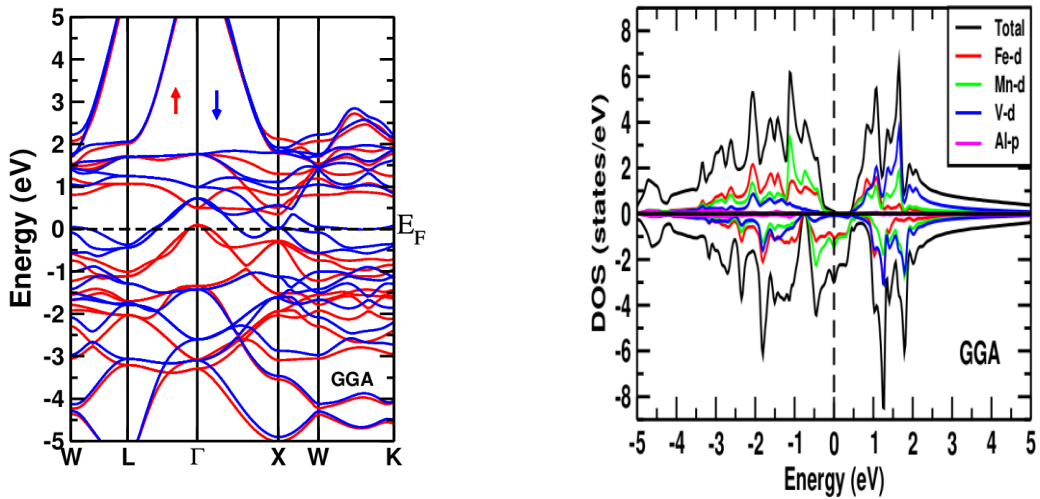


FIG. 3. (Color online) (a) The band structure of FeMnVAI for spin-up (red) and spin-down (blue) channels and (b) DOS plot under the GGA technique.

Figure shows that there is a gap around the Fermi level in the spin up channel, whereas in the down spin channel, the conduction and valence bands are crossing near the Fermi level, indicating half-metallic behaviour of the compound. It is observed that the valence band (VB) maxima appears slightly above the Fermi

level at the Γ symmetric point in the up spin channel. The clear gap is observed in up spin channel from the corresponding DOS plot. As a result, under the GGA approach, the compound (FeMnVAI) exhibits metallic behaviour in the down spin channel and nearly semiconducting behaviour in the up spin

channel. The contributions of DOS for the half metallicity is in the order of $Mn_d > Fe_d > V_d$.

The electronic properties of FeMnVAI compound were also examined using mBJ and GGA+U techniques. Under the mBJ method and GGA+U method, the Fermi energy level seems more enhance and clear. The mBJ method revealed a clear energy gap around the Fermi level in the spin-up channel(0.605 eV), indicating semiconducting behavior, while the spin-down channel showed metallic characteristics (Fig. 4 a, b) . Similarly, the GGA+U method also demonstrated half-metallic

behavior with 0.314 eV gap at spin up channel (Fig 5 a, b). Additionally, analysis of the density of states (DOS) plots corroborated these findings, showing nearly semiconducting behavior in the spin-up channel and metallic behavior in the spin-down channel under both the mBJ and GGA+U methods. Overall, FeMnVAI exhibits true half-metallic nature, as confirmed by multiple computational methods and electronic structure analyses. There is no change in the ratio of the contributions observed from projected DOS while moving from GGA to mBJ and GGA+U.

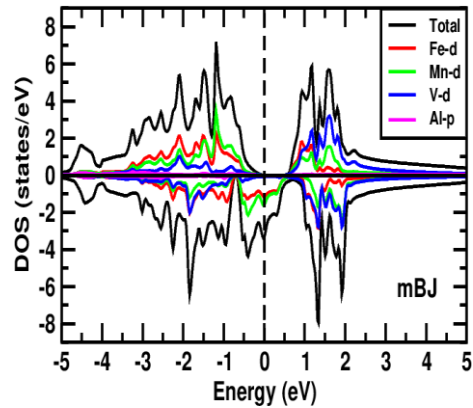
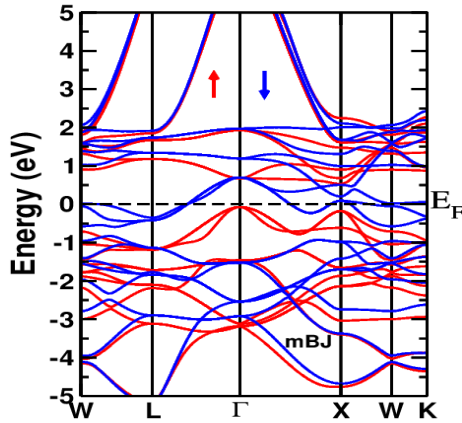


FIG. 4. (Color online) The band structure of FeMnVAI for spin-up (red) and spin-down (blue) channels under the mBJ technique.

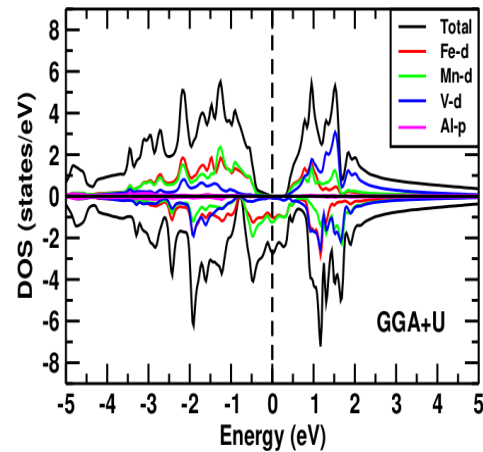
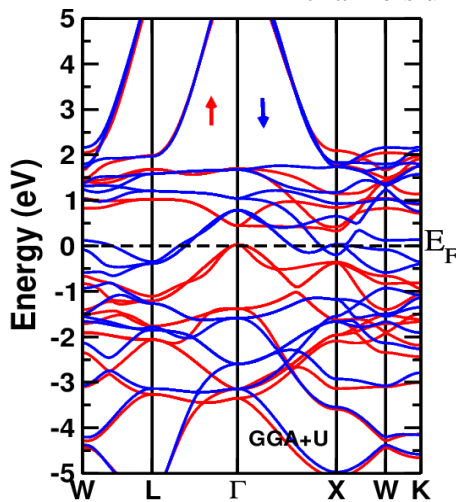


FIG. 5. (Color online) The band structure of FeMnVAI for spin-up (red) and spin-down (blue) channels under the GGA+U technique.

C: Magnetic properties

The study on FeMnVAI compound reveals its magnetic nature through asymmetrical density of states (DOS) for up and down spin channels. Total spin magnetic moments, calculated using under GGA, mBJ and GGA+U techniques which shows almost an integer value $1.00 \mu_B$ in

TABLE III: Total magnetic moments $\mu_{\text{total}}(\mu_B/\text{f.u.})$ and atomic magnetic moments $\mu_{\text{atomic}}(\mu_B/\text{f.u.})$ of FeMnVAI under the GGA, mBJ and GGA+U techniques.

Alloy	μ_{total}	μ_{Fe}	μ_{Mn}	μ_{V}	μ_{Al}	VBM	CBM	E_{bg}
FeMnVAI ^{GGA}	0.991	0.608	0.914	-0.457	-0.011	0.087	0.344	0.257
FeMnVAI ^{mBJ}	0.999	0.654	1.006	-0.557	-0.019	-0.081	0.524	0.605
FeMnVAI ^{GGA+U}	0.999	0.671	1.173	-0.705	-0.023	0.010	0.324	0.314

The spin polarization (P) will be analyzed using DOS of up spin and down spin electrons at the Fermi level using a relation:

$$P = \frac{n_{\uparrow}(E_F) - n_{\downarrow}(E_F)}{n_{\uparrow}(E_F) + n_{\downarrow}(E_F)} \quad (11)$$

where $n_{\uparrow}(E_F)$ and $n_{\downarrow}(E_F)$ represents the DOS at the Fermi level for the majority (spin up) and minority (spin down) states respectively. The electrons are fully polarized, when $n_{\uparrow}(E_F)$ or $n_{\downarrow}(E_F)$ is equal to zero. The results of spin polarization indicates that FeMnVAI is 100 % spin polarized.

IV. CONCLUSIONS

We investigated the structural, mechanical, electronic, and magnetic properties of FeMnVAI alloys using GGA, mBJ, and GGA+U techniques. Structural optimization identified the stable type I structure with a ferromagnetic (FM) state. Negative values for formation and cohesive energies confirm the compound's chemical stability. The equilibrium lattice

all techniques (Table IV), which meet with the Slater-Pauling rule $M_t = Z_t - 24$, where M_t and Z_t represents total magnetic moment and total number of valence electrons of the compound [53,54]. The positive magnetic moments in Fe and Mn dominate suggesting ferromagnetic behavior of compound.

constant of FeMnVAI was found to be 5.757 \AA . Mechanical stability was confirmed by Born-Huang conditions, while mechanical parameters indicate ductile behavior. Electronic structure analysis revealed nearly half-metallic (HM) behavior under GGA and true HM nature under mBJ and GGA+U techniques. The computed magnetic moment of FeMnVAI, close to $1.00 \mu_B/\text{f.u.}$, adheres to the Slater-Pauling rule ($M_t = Z_t - 24$), where where M_t and Z_t represents total magnetic moment and total number of valence electrons of the compound. Such properties of the compounds are suitable for optoelectronic as well as spintronics device applications.

V. ACKNOWLEDGMENT

R.B.R. is thankful to Rector office, T.U., University Grants Commission (UGC) and Nepal Academy of Science and Technology (NAST), Nepal for partial financial support.

References:

- [1] R.A. de Groot, F.M. Mueller, P.G. Van Engen, and K.H.J. Buschow, New class of materials: half-metallic ferromagnets, *Phys. Rev. Lett.* 50, 2024 (1983).
- [2] S. Berri, First-principles study on half-metallic properties of the CoMnCrSb quaternary Heusler compound, *J. Supercond. Nov. Magnet.* 29, 1309 (2016).
- [3] Z. H. Xiong, D. Wu, Z.V. Vardeny, J. Shi, Giant magnetoresistance in organic spin-valves, *Nature* 427, 821 (2004).
- [4] D. Kurebayashi, K. Nomura, Theory for spin torque in Weyl semimetal with magnetic texture, *Sci. Rep.* 9, 5365(2019).
- [5] L. Bainsla, K.Z. Suzuki, M. Tsujikawa, H. Tsuchiura, M. Shirai, S. Mizukami, Magnetic tunnel junctions with an equiatomic quaternary CoFeMnSi Heusler alloy electrode, *Appl. Phys. Lett.* **112**, 052403 (2018).
- [6] I. Zutic, J. Fabian, S. D. Sharma, Spintronics: fundamentals and applications, *Rev. Mod. Phys.* **76**, 323(2004).
- [7] Y. K. Takahashi, S. Kasai, S. Hirayama, S. Mitani and K. Hono, All-metallic lateral spin valves using Co₂Fe (Ge_{0.5} Ga_{0.5}) Heusler alloy with a large spin signal, *Appl. Phys. Lett.* 100, 052405(2012).
- [8] S. Wurmehl, G.H. Fecher, H. C. Kandpal, V. Ksenofontov, C. Felser and H.J. Lin, Investigation of Co₂FeSi: The Heusler compound with highest Curie temperature and magnetic moment, *Appl. Phys. Lett.* 88 032503 (2006).
- [9] P. Wang, J. Xia, H. Wu, Electronic structures, magnetic properties and strain effects of quaternary Heusler alloys FeMnCrZ (Z = P, As, Sb, Bi, Se, Te), *J. Magn. Magn. Mater.* 490 165490(2019).
- [10] G.Y. Gao, L. Hu, K.L. Yao, B. Luo, N. Liu, Large half-metallic gaps in the quaternary Heusler alloys CoFeCrZ (Z = Al, Si, Ga, Ge): a first-principles study, *J. Alloy. Compd.* 551, 539 (2013).
- [11] L. Zhang, Z. X. Cheng, X. T. Wang, R. Khenata, H. Rozale, First-principles investigation of equiatomic quaternary Heusler alloys NbVMnAl and NbFeCrAl and a discussion of the generalized electron-filling rule, *J. Supercond. Nov. Magnet.* 31, 189(2018).
- [12] Y. Du, G. Z. Xu, E. K. Liu, G. J. Li, H. G. Zhang, S. Y. Yu, W. H. Wang and G. H. Wu, Crossover of magnetoresistance in the zero-gap half-metallic Heusler alloy Fe₂CoSi, *J. Magn. Magn. Mater.* **335**,101(2013).
- [13] X. F. Dai, G. D. Liu, G. H. Fecher, C. Felser, Y. X. Li and H. Y. Liu, New quaternary half metallic material CoFeMnSi, *J. Appl. Phys.* 105 , 07E901(2009).
- [14] R. Y. Umetsu, K. Kobayashi, R. Kainuma, A. Fujita, K. Fukamichi, K. Ishida and A. Sakuma, Magnetic properties and band structures of half-metal type Co₂CrGa

- Heusler alloy, *Appl. Phys. Lett.* 85, 2011(2004).
- [15] D. K. Yadav, S. R. Bhandari, G. C. Kaphle, Structural, elastic, electronic and magnetic properties of MnNbZ (Z = As, Sb) and FeNbZ (Z = Sn, Pb) semi-Heusler alloys, *Mater. Res. Express* 7, 116527(2020).
- [16] R. Paudel, G.C. Kaphle, M. Batouche, J. Zhu, Halfmetallicity, magnetism, mechanical, thermal, and phonon properties of FeCrTe and FeCrSe half-Heusler alloys under pressure, *J. Quantum Chem.*, 120, e26417(2020).
- [17] N. Mehmood, R. Ahmad, Structural, electronic, magnetic, and optical properties of half-Heusler alloys RuMnZ (Z = P, As): a first-principle study, *J. Supercond. Nov. Magnet.* 31, 233(2018).
- [18] E. G. Ozdemir, Z. Merdan, First principle predictions on half-metallic results of MnZrX (X = In, Tl, C, Si, Ge, Sn, Pb, N, P, As, Sb, O, S, Se, Te) half-Heusler compounds, *J. Magn. Mater.* 491, 165567 (2019).
- [19] R. Dhakal, S. Nepal, R.B. Ray, R. Paudel, G.C. Kaphle, Effect of doping on SGS and weak half-metallic properties of inverse Heusler alloys, *J. Magn. Mater.* 503, 166588. (2020)
- [20] L. Jia, L. Yangxian, Z. Cuoxing, S. Yubao, S. Q. Chang, A first principles study on the full-Heusler compound Cr₂MnAl, *Appl. Phys. Lett.* 94, 24250(2009).
- [21] L. Hongzhi, Z. Zhu, L. Ma, S. Xu, Electronic structure and magnetic properties of Fe₂YSi (Y = Cr, Mn, Fe, Co, Ni) Heusler alloys: a theoretical and experimental study, *J. Phys. D Appl. Phys.* 40, 7121(2007).
- [22] S. Cherid, W. Benstaali, A. Abbad, S. Bentata, T. Lantri, A. Boucif, Theoretical prediction of half-metallic ferromagnetic full-Heusler alloys Cs₂CrGe, *Solid State Commun.* 260, 14(2017).
- [23] I. Galanakis, Appearance of half-metallicity in the quaternary Heusler alloys, *J. Phys. Condens. Matter* 16, 3089(2004).
- [24] G. Y. Gao, L. Hu, K.L. Yao, B. Luo, N. Liu, Large half-metallic gaps in the quaternary Heusler alloys CoFeCrZ (Z = Al, Si, Ga, Ge): a first-principles study, *J. Alloy. Compd.* 551, 539(2013).
- [25] V. Alijani, J. Winterlik, G.H. Fecher, S.S. Naghavi, C. Felser, Quaternary half-metallic Heusler ferromagnets for spintronics applications, *Phys. Rev.B* 83, 184428.(2011)
- [26] L. Zhang, Z. X. Cheng, X. T. Wang, R. Khenata, H. Rozale, First-principles investigation of equiatomic quaternary Heusler alloys NbVMnAl and NbFeCrAl and a discussion of the generalized electron-filling rule, *J. Supercond. Nov. Magnet.* 31, 189 (2018).
- [27] B. Regmi, G. C. Kaphle, R. B. Ray, D. Paudyal, Unraveling peculiar magnetism and band topology in Mn₃Sb, *J. Alloy.*

- Compd. 891, 162024(2022).
- [28] S. Bahramian, F. Ahmadian, Half-metallicity and magnetism of quaternary Heusler compounds CoRuTiZ ($Z = \text{Si, Ge, and Sn}$), *J. Magn. Magn. Mater.* **424**, 122(2017).
- [29] Q. Zhang, P. Xie, C. Liu, S. Li, X. Lie et al., Enhanced thermoelectric performance of Hafnium free n-type ZrNiSn half-Heusler alloys by isoelectronic Si substitution, *Materials Today Phys.* **24**, 100648 (2022).
- [30] X. Dai, G. Liu, G. H. Fecher, C. Felser, Y. Li, and H. Liu, New quaternary half metallic material CoFeMnSi , *Appl. Phys. Lett.* **104**, 172407 (2014).
- [31] B. Pandey, R. B. Ray, and G. C. Kaphle, First-principles study of structural, electronic, and magnetic properties of Co-doped quaternary Heusler compounds. *Bibechana*, 15, 50-50 (2018).
- [32] M. Mushtaq, M.A. Sattar, Sajad Ahmad Dar, I. Qasim, I. Muhammad, Search for half-metallicity in new ferri-magnetic quaternary MnXMoAl ($X = \text{Co and Ti}$) Heusler alloys: A DFT based investigation, *Materials Chemistry and Physics* 245 122779(2020).
- [33] R. B. Ray, G. C. Kaphle, R. K. Rai, D. K. Yadav, R. Paudel, D. Paudyal, Strain induced electronic structure, and magnetic and structural properties in quaternary Heusler alloys ZrRhTiZ ($Z = \text{Al, In}$) *J. Alloy. Compd.* **867**, 158906(2021).
- [34] K. Schwarz, P. Blaha, Georg K.H. Madsen, Electronic Structure Calculations of Solids Using the WIEN2k Package for Material Sciences, *Solid State Commun.* **270** 111 (2018).
- [35] P. Blaha, K. Schwarz, P. Sorantin, S. B. Trickey, Full-potential, linearized augmented plane wave programs for crystalline systems, *Comput. Phys. Commun.* **59**, 399(1990).
- [36] W. Kohn and L. J. Sham, Self-consistent equations including exchange and correlation effects, *Phys. Rev.* 140, 1133(1965).
- [37] P. Hohenberg, W. Kohn, Density functional theory, *Phys. Rev.* **136**, 864(1964).
- [38] V. I. Anisimov and O. Gunnarsson, Density functional calculation of effective Coulomb interactions in metals, *Phys. Rev. B* 43, 7570(1991).
- [39] J. P. Perdew, K. Burke, Y. Wang, Generalized gradient approximation for the exchange-correlation hole of a many-electron system, *Phys. Rev. B* 54, 16533(1996).
- [40] D. Koller, F. Tran, P. Blaha, Improving the modified Becke-Johnson exchange potential, *Phys. Rev. B* 85 155109(2012).
- [41] A. D. Becke, E. R. Johnson, A simple effective potential for exchange, *J. Chem. Phys.* 124 221101(2006).
- [42] F. Aryasetiawan, K. Karlsson, O. Jepsen, U.

- Schonberger, Calculations of Hubbard U from first-principles, *Phys. Rev. B* **74** 125106(2006).
- [43] K. Karlsson, F. Aryasetiawan, O. Jepsen, Method for calculating the electronic structure of correlated materials from a truly first-principles LDA+U scheme, *Phys. Rev. B* **81**, 245113(2010) .
- [44] E. Sasioglu, I. Galanakis, Ch. Friedrich and S. Blgel, Ab initio calculation of the effective on-site Coulomb interaction parameters for half-metallic magnets *PHYSICAL REVIEW B* **88** ,134402(2013) .
- [45] P. Blaha, K. Schwarz, G. K. H. Madsen, D. Hvasnicka D, J. Luitz and K Schwarz 2001 WIEN2k An Augmented Plane Wave Local Orbitals Program for Calculating Crystal Properties (Austria: Techn. Univ. Wien)
- [46] M. Attallah, M. Ibrir, S. Berri, S. Lakel, Ab initio study of electronic structure and magnetic properties of CoMnTaZ (Z = Si, Ge) quaternary Heusler compounds, *Physica Status Solidi*. 14, 1700127 (2017).
- [47] R. Paudel and J. Zhu, Investigation of half-metallicity and magnetism of (Ni/Pd/Ru) ZrTiAl quaternary Heusler alloys for spintronic applications, *Physica B Condens. Matter* **557**, 45(2019).
- [48] F. D. Murnaghan, The Compressibility of Media under Extreme Pressures, *Proc. Natl. Acad. Sci.* **30**, 244(1944).
- [49] P. Wang, J. B. Xia, H. B. Wu, Electronic structure, magnetic properties and strain effects of quaternary Heusler alloys FeMnCrZ (Z = P, As, Sb, Bi, Se, Te), *J. Magn. Magn. Mater.* **490**, 165490 (2019).
- [50] S. Nepal, R. Dhakal, I. Galanakis, S. M. Winter, R. P. Adhikari, and G. C. Kaphle, Ab initio study of stable 3d, 4d, and 5d transition-metal-based quaternary Heusler compounds, *Phys. Rev. Materials* **6**, 114407 (2022)
- [51] L. Zuo, M. Humbert, C. Esling, Elastic properties of polycrystals in the Voigt-Reuss-Hill approximation, *J. Appl. Crystallogr.* 25 751(1992).
- [52] S. F. Pugh, XCII. Relations between the elastic moduli and the plastic properties of polycrystalline pure metals, *Lond. Edinb. Dublin Philos. Mag. J. Sci.* **45**, 823 (1954).
- [53] B Pandey, R. B. Ray, G. C. Kaphle, First-principles study of structural, electronic and magnetic properties of Co-based quaternary Heusler compounds: CoFeCrAl, CoFeTiAs, CoFeCrGa and CoMnVAs, *BIBECHANA* **15** , 50-59 (2018) .
- [54] R. Jain, V. K. Jain, A. R. Chandra, V. Jain, N. Lakshmi, Study of the Electronic Structure, Magnetic and Elastic Properties and Half-Metallic Stability on Variation of Lattice Constants for CoFeCrZ (Z = P, As, Sb) Heusler Alloys. *J. Supercond. Nov. Magn.* **31**, 2399(2018).